Toward improved boundary conditions for the DNS and LES of turbulent subsonic flows

By R. Prosser† and J. Schlüter

A procedure is outlined for the specification of time dependent boundary conditions, suitable for viscous, conducting flows. The method is based on a low Mach number asymptotic expansion of the governing equations and the characteristics derived from them. By consistent matching of the terms in the expansions, it is possible to develop inflow and outflow conditions that are transparent to acoustic waves, yet retain the flexibility to allow for complex flow structures such as turbulence to enter or leave the computational domain. The boundary conditions developed here represent a midway point in the evolution of this approach, which was originally developed for Euler flows, and which is evolving toward treatment of fully reacting viscous simulations.

1. Introduction

The specification of appropriate boundary conditions for compressible, turbulent reacting flows is an open problem. Even for simplified flows, such as those without thermal conduction or chemical effects, the structure of a turbulent flow is complex. The specification of time dependent boundary conditions for such flows poses a challenge to many of the currently available methods, which themselves are essentially based on the linearized Euler equations.

Broadly speaking, boundary conditions fall into two categories: *global methods* and *local methods*. In the former category transforms are taken of the governing equations, and the boundary conditions are expressed in terms of a non-local asymptotic expression designed to admit the passage of wave-like phenomena (Tsynkov 1998). The family of global methods are difficult to implement in general flows however, and there are still significant uncertainties regarding their application to flows with chemical reactions and heat release. The second family of methods obtain boundary conditions by exploiting information derived from the local behaviour of the flow. A number of authors have used local methods to derive non-reflecting boundary conditions, such as the PML approach (Hu 1996; Hesthaven 1998) and the family of schemes based on the method of characteristics. This latter class is particularly popular, and although originally designed for the linearized Euler system (Thompson 1987; Vichnevetsky 1986; Hedstrom 1979; Rudy & Strikwerda 1981; Rudy & Strikwerda 1980), the methods have been developed considerably. The culmination of these efforts is found in the **N**avier-**S**tokes **C**haracteristic **B**oundary **C**onditions (NSCBC) and the **L**ocal **O**ne **D**imensional **I**nviscid (LODI) approaches developed by Poinsot and Lele (Poinsot & Lele 1992). This method has been demonstrated in a number of challenging flow cases, such as the free shear layer simulations of Grinstein (Grinstein 1994), for the short time integration of low Mach number flows. The NSCBC approach has been further modified for reacting flows by Baum,

† Dept. of Mechanical, Aerospace and Manufacturing Engineering UMIST, Manchester, UK

Poinsot and Thévenin (Baum *et al.* 1994; Thevénin *et al.* 1996), and more recently by Sutherland and Kennedy (Sutherland & Kennedy 2003). Recently, Nicoud (Nicoud 1999) has developed the LODI approach to provide a promising avenue toward the generation of acoustically transparent inflow conditions. In the LODI approach, the hyperbolic components of the governing equations are decomposed into characteristics at the computational boundary. If the required boundary specification is to be non-reflecting, then the amplitude time variation of the incoming characteristics are set to zero (Hedstrom 1979). The LODI mechanism provides a means of specifying Dirichlet or Neumann boundary conditions via the balancing of the incoming and outgoing characteristics. While elegant, the LODI/NSCBC approach has the drawback that (at this time), the scheme still prevents the specification of acoustically transparent, non-trivial inflow boundary conditions. Simultaneously, the method has some difficulty in representing the pressure field accurately when turbulence crosses the computational domain (Prosser 2004). The work described here builds on results obtained previously for inviscid flows (Prosser 2004), and aims to produce non-reflecting boundary conditions for non-reacting viscous, conducting flows. The extension of the method to the viscous reacting flow case will be described in a future paper.

2. The governing equations

In a domain $\Omega \subset \mathbf{R}^n$, the compressible Navier-Stokes equations can be written as

$$\partial_t \left(\widetilde{\mathbf{U}}\right) + \sum_{i=1}^{n} \partial_{\widetilde{x}_i} \left(\mathbf{F}_i\right) = \mathbf{C}, \tag{2.1}$$

where $\widetilde{\mathbf{U}}$ is the $n+2$ dimensional vector of conserved variables, $\mathbf{F}_i$ is the $n+2$ dimensional flux vector and $\mathbf{C}$ is a vector containing diffusive fluxes, reaction rates and other algebraic terms.

For a boundary whose normal points in the x_α direction, the NSCBC approach decomposes the $\alpha-$direction flux term into

$$\partial_t \left(\widetilde{\mathbf{U}}\right) + \mathbf{P}\mathbf{S}_\alpha^{-1}\Lambda_\alpha \mathbf{S}_\alpha \partial_{\widetilde{x}_\alpha} \left(\mathbf{U}\right) + \sum_{\substack{i=1 \\ i\neq\alpha}}^{n} \partial_{\widetilde{x}_i} \left(\mathbf{F}_i\right) = \mathbf{C}. \tag{2.2}$$

In equation system 2.2, $\mathbf{U}$ is a (non-unique) vector of primitive variables, $\mathbf{P} = \widetilde{\mathbf{U}}_{\mathbf{U}}$, Λ_α is the diagonal matrix of eigenvalues of $\mathbf{P}^{-1}\left(\left(\mathbf{F}_\alpha\right)_{\mathbf{U}}\right)$, and $\mathbf{S}_\alpha$ is the matrix of left eigenvalues of $\mathbf{P}^{-1}\left(\mathbf{F}_\alpha\right)_{\mathbf{U}}$. There is no summation over Greek indices. The equivalent primitive formulation to equation system 2.2 is

$$\partial_t \left(\mathbf{U}\right) + \mathbf{S}_\alpha^{-1}\Lambda_\alpha \mathbf{S}_\alpha \partial_{\widetilde{x}_\alpha} \left(\mathbf{U}\right) + \sum_{\substack{i=1 \\ i\neq\alpha}}^{n} \mathbf{P}^{-1}\left(\mathbf{F}_i\right)_{\mathbf{U}} \partial_{\widetilde{x}_i} \left(\mathbf{U}\right) = \mathbf{P}^{-1}\mathbf{C}. \tag{2.3}$$

In the literature on NSCBC boundary conditions the nomenclature $\mathbf{L}_\alpha = \Lambda_\alpha \mathbf{S}_\alpha$ is often used, with $\mathbf{L}_\alpha$ referred to as the vector of *characteristic wave amplitude variations* (or *amplitudes* hereafter). In the following, we extend the treatment developed by Prosser (Prosser 2004) for Euler flows, to include the effects of molecular transport on the specification of these amplitudes.

We begin by considering a two-dimensional problem ($n = 2$). We non-dimensionalise equation systems 2.2 and 2.3, and introduce a low Mach number expansion for each

of the dependent variables (McMurtry *et al.* 1986) i.e. the pressure is written as $p = p^{(0)} + Mp^{(1)} + M^2 p^{(2)} + O\left(M^3\right)$. Bracketed, superscripted numbers are used to index the terms in a given expansion. The second step is to decompose the convective flux terms into motions defined on two length scales: inertial scales $\mathbf{x} = (x\ y)^T$ and acoustic scales $\eta = (\xi\ \theta)^T$, $\xi = Mx$, $\theta = My$. The convective derivatives appearing in the Navier-Stokes equations are consequently expressed as (in the case of the non-dimensionalised $\widetilde{x}$ derivative (Klein 1995))

$$\left.\frac{\partial}{\partial \widetilde{x}}\right|_{M,t} = \frac{\partial}{\partial x} + M\frac{\partial}{\partial \xi}. \tag{2.4}$$

The expansions are inserted into the primitive equations and the associated characteristics. By appropriate matching of terms, revised treatments for time dependant boundary conditions can be derived that better satisfy the demands of mass, momentum and energy conservation.

For the choice of conservative vector $\widetilde{\mathbf{U}} = (\rho\ \rho u\ \rho v\ \rho E)^T$, the dimensionless form of the equation system for a viscous, conducting, single species flow is written as

$$\begin{aligned}
\frac{\partial \rho}{\partial t} + \frac{\partial}{\partial \widetilde{x}_k}\left(\rho u_k\right) &= 0 \\
\frac{\partial \left(\rho u_i\right)}{\partial t} + \frac{\partial}{\partial \widetilde{x}_k}\left(\rho u_i u_k\right) + \frac{1}{M^2}\frac{\partial p}{\partial \widetilde{x}_k} &= \frac{1}{\mathrm{Re}}\frac{\partial \tau_{ik}}{\partial \widetilde{x}_k} \\
\frac{\partial \left(\rho E\right)}{\partial t} + \frac{\partial}{\partial \widetilde{x}_k}\left(\left(\rho E + p\right) u_k\right) &= \frac{\left(\gamma - 1\right) M^2}{\mathrm{Re}}\frac{\partial}{\partial \widetilde{x}_k}\left(u_i \tau_{ik}\right) \\
&+ \quad \frac{1}{\mathrm{Re}\,\mathrm{Pr}}\frac{\partial}{\partial \widetilde{x}_k}\left(\lambda \frac{\partial T}{\partial \widetilde{x}_k}\right).
\end{aligned} \tag{2.5}$$

In the previous equations, $\widetilde{x}_i$ represents the dimensionless distance. Re is the flow Reynolds number. E is the stagnation internal energy, τ is the viscous stress tensor and M is a flow Mach number (defined below). Pr is the Prandtl number and λ is the thermal conductivity. The equations are closed by the thermal and caloric equations of state;

$$p = \rho R T \tag{2.6}$$

$$h = h^0 + \int c_p\left(T'\right) dT'. \tag{2.7}$$

In equations 2.5a-c, the variables have been non-dimensionalised with respect to a length scale characterising the domain size l_0, a density ρ_0 and a velocity u_0, which is assumed to be small with respect to the local sound speed. Under these assumptions, the flow Mach number $u_0\left(\gamma R_0 T_0\right)^{-\frac{1}{2}}$ appearing in equations 2.5b and 2.5c is small. The thermodynamic quantities c_p, c_v, and R, (which henceforth will be assumed to be constant) are non-dimensionalized with respect to $\left(c_p\right)_0 \equiv c_p$. The pressure is non-dimensionalized with respect to a thermodynamic pressure $\gamma \rho_0 R T_0$, where T_0 is an absolute temperature and γ is introduced to simplify the subsequent algebra. Using these variables, the local sound speed in dimensionless coordinates is $a = M^{-1}\left(\gamma p/\rho\right)^{\frac{1}{2}}$. Finally, we introduce a supplementary equation for the pressure as this is will be useful in the later development;

$$\frac{\partial p}{\partial t} + u_k\frac{\partial p}{\partial \widetilde{x}_k} + \gamma p\left(\frac{\partial u_k}{\partial \widetilde{x}_k}\right) = \frac{\left(\gamma - 1\right) M^2}{\mathrm{Re}}\tau_{ik}\frac{\partial u_i}{\partial \widetilde{x}_k} + \frac{1}{\mathrm{Re}\,\mathrm{Pr}}\frac{\partial}{\partial \widetilde{x}_k}\left(\lambda \frac{\partial T}{\partial \widetilde{x}_k}\right). \tag{2.8}$$

equation 2.8 can be derived from equations 2.5a-c, 2.6 and 2.7, and can be used in place of equation 2.5c if desired (Majda & Sethian 1985).

For definiteness, we consider a two dimensional domain whose boundaries are aligned with the $\widetilde{x}$ and $\widetilde{y}$ axes. We assume that the left hand (inlet) boundary will be located at $\widetilde{x} = 0$, the right hand (outlet) boundary will be located at $\widetilde{x} = 1$. Using the methods outlined above, the governing equations are consequently replaced on the boundaries by

$$\begin{aligned}
\frac{\partial \rho}{\partial t} &= -\left(\frac{\rho}{T}\left(L_1 + L_4\right) - \frac{\rho}{c_p}L_2 + v\frac{\partial \rho}{\partial \widetilde{y}} + \rho\frac{\partial v}{\partial \widetilde{y}}\right) \\
\frac{\partial u}{\partial t} &= -\left(\frac{1}{MT}\sqrt{\frac{\gamma p}{\rho}}\left(L_4 - L_1\right) + v\frac{\partial u}{\partial \widetilde{y}}\right) + \frac{1}{\mathrm{Re}}\left(\frac{\partial \tau_{\widetilde{x}\widetilde{x}}}{\partial \widetilde{x}} + \frac{\partial \tau_{\widetilde{x}\widetilde{y}}}{\partial \widetilde{y}}\right) \\
\frac{\partial v}{\partial t} &= -\left(L_3 + v\frac{\partial v}{\partial \widetilde{y}} + \frac{1}{\rho M^2}\frac{\partial p}{\partial \widetilde{y}}\right) + \frac{1}{\mathrm{Re}}\left(\frac{\partial \tau_{\widetilde{y}\widetilde{x}}}{\partial \widetilde{x}} + \frac{\partial \tau_{\widetilde{y}\widetilde{y}}}{\partial \widetilde{y}}\right) \\
\frac{\partial p}{\partial t} &= -\left(\rho c_p\left(L_4 + L_1\right) + \gamma p\frac{\partial v}{\partial \widetilde{y}} + v\frac{\partial p}{\partial \widetilde{y}}\right) \\
&\quad + \frac{\left(\gamma - 1\right)M^2}{\mathrm{Re}}\Phi + \frac{1}{\mathrm{Re}\,\mathrm{Pr}}\left(\frac{\partial}{\partial \widetilde{x}}\left(\lambda\frac{\partial T}{\partial \widetilde{x}}\right) + \frac{\partial}{\partial \widetilde{y}}\left(\lambda\frac{\partial T}{\partial \widetilde{y}}\right)\right)
\end{aligned} \tag{2.9}$$

in which $\Phi \equiv \tau : \nabla u \geq 0$, and the dimensionless specific heats $c_p\,(\equiv 1)$ and $c_v\,\left(\equiv \gamma^{-1}\right)$ are kept explicitly to help clarify the algebra when the equations are re-expressed in their dimensional form. The amplitudes are

$$\begin{aligned}
L_1 &= \frac{1}{2\rho c_p}\left(u - \frac{1}{M}\sqrt{\frac{\gamma p}{\rho}}\right)\left(\frac{\partial p}{\partial \widetilde{x}} - M\sqrt{\gamma \rho p}\frac{\partial u}{\partial \widetilde{x}}\right) \\
L_2 &= u\left(c_v\left(\frac{1}{p}\frac{\partial p}{\partial \widetilde{x}} - \frac{\gamma}{\rho}\frac{\partial \rho}{\partial \widetilde{x}}\right)\right) \\
L_3 &= u\frac{\partial v}{\partial \widetilde{x}} \\
L_4 &= \frac{1}{2\rho c_p}\left(u + \frac{1}{M}\sqrt{\frac{\gamma p}{\rho}}\right)\left(\frac{\partial p}{\partial \widetilde{x}} + M\sqrt{\gamma \rho p}\frac{\partial u}{\partial \widetilde{x}}\right)
\end{aligned} \tag{2.10}$$

At the inlet boundary, conditions must be specified for the unknown incoming amplitudes; L_2, L_3, L_4. For the outlet boundary, the only incoming amplitude requiring specification is L_1. Traditional non-reflecting boundary conditions (Hedstrom 1979; Thompson 1987) are obtained by setting all incoming amplitudes to zero. A range of other practical boundary conditions can be specified by appropriate matching of incoming or outgoing amplitudes (Poinsot & Lele 1992; Baum *et al.* 1994). It has been previously demonstrated (Prosser 2004) that these older boundary conditions produce spurious pressure oscillations that propagate into the computational domain at the local speed of sound. This is

because, for low Mach number flows, the non-linear amplitudes have the expansions

$$\begin{aligned} L_1 &= L_1^{(0)} + ML_1^{(1)} + \dots \\ &= \frac{1}{2\rho^{(0)}c_p}\left(\gamma p^{(0)}\frac{\partial u^{(0)}}{\partial x} + M\left(\gamma p^{(0)}\left(\frac{\partial u^{(0)}}{\partial \xi} + \frac{\partial u^{(1)}}{\partial x} + \frac{\partial u^{(0)}}{\partial x}\left(\frac{p^{(1)}}{p^{(0)}} - \frac{\rho^{(1)}}{\rho^{(0)}}\right)\right)\right.\right. \\ &\quad \left.\left. - \sqrt{\frac{\gamma p^{(0)}}{\rho^{(0)}}}\left\{\frac{\partial p^{(1)}}{\partial \xi} + \frac{\partial p^{(2)}}{\partial x} + \rho^{(0)}u^{(0)}\frac{\partial u^{(0)}}{\partial x}\right\}\right)\right) + O\left(M^2\right) \end{aligned} \tag{2.11}$$

$$\begin{aligned} L_4 &= L_4^{(0)} + ML_4^{(1)} + \dots \\ &= \frac{1}{2\rho^{(0)}c_p}\left(\gamma p^{(0)}\frac{\partial u^{(0)}}{\partial x} + M\left(\gamma p^{(0)}\left(\frac{\partial u^{(0)}}{\partial \xi} + \frac{\partial u^{(1)}}{\partial x} + \frac{\partial u^{(0)}}{\partial x}\left(\frac{p^{(1)}}{p^{(0)}} - \frac{\rho^{(1)}}{\rho^{(0)}}\right)\right)\right.\right. \\ &\quad \left.\left. + \sqrt{\frac{\gamma p^{(0)}}{\rho^{(0)}}}\left\{\frac{\partial p^{(1)}}{\partial \xi} + \frac{\partial p^{(2)}}{\partial x} + \rho^{(0)}u^{(0)}\frac{\partial u^{(0)}}{\partial x}\right\}\right)\right) + O\left(M^2\right). \end{aligned} \tag{2.12}$$

By comparing the leading order terms of L_1 and L_4 with the leading order expansion of equation 2.8, it can be seen that the amplitudes control the value of the global thermodynamic pressure (via the maintenance of a divergence free velocity field). Similarly, the momentum equation—which appears in the above equations as an $O(M)$ term—must also be retained for correct treatment of the momentum at the boundary. Consequently, we seek a new treatment for L_1 and/or L_4 that retains these essential features, but still keeps the non-reflecting behaviour.

3. Revised viscous outflow boundary conditions

A natural first step towards a revised outflow is to generalise the LODI/NSCBC boundary condition of Poinsot *et al.* (Poinsot & Lele 1992; Thevénin *et al.* 1996; Baum *et al.* 1994) to flows with transverse inertial structure and viscosity. We re-write equation 2.9b in terms of the leading orders of a low Mach number expansion and rearrange to obtain

$$L_1 = L_4 - MT^{(0)}\sqrt{\frac{\rho^{(0)}}{\gamma p^{(0)}}}\left(\frac{1}{\mathrm{Re}}\left(\frac{\partial \tau_{yx}^{(0)}}{\partial x} + \frac{\partial \tau_{yy}^{(0)}}{\partial y}\right) - \frac{\partial u^{(0)}}{\partial t} - v\frac{\partial u^{(0)}}{\partial y}\right) + O\left(M^2\right). \tag{3.1}$$

There are two difficulties with equation 3.1: the specification of $\partial u^{(0)}/\partial t$, and the reflecting nature of the resulting boundary condition. There are a number of ways to deal with the temporal term. For the purposes of this paper, we use a simple frozen turbulence approximation:

$$\frac{\partial u^{(0)}}{\partial t} = -u_b\frac{\partial u^{(0)}}{\partial x}, \tag{3.2}$$

where u_b is the mean speed of the flow. To deal with the reflection, we realise that the boundary is reflective because L_1 should contain *only* left-going acoustic waves, while L_4 contains *only* right going waves (c.f. equations 2.11 and 2.12). Equating the two directly leads to L_1 inheriting a wave propagating in the wrong direction (Prosser 2004). The non-reflecting condition translates to the absence of incoming acoustic waves at the boundary and hence, equation 3.1 should have all acoustic behaviour removed from it.

This is achieved explicitly by subtracting the acoustic component of L_4 to obtain

$$L_1 = L_4 - MT^{(0)}\sqrt{\frac{\rho^{(0)}}{\gamma p^{(0)}}}\left(\frac{1}{\mathrm{Re}}\left(\frac{\partial \tau_{yx}^{(0)}}{\partial x}+\frac{\partial \tau_{yy}^{(0)}}{\partial y}\right)+u_b\frac{\partial u^{(0)}}{\partial x}-v\frac{\partial u^{(0)}}{\partial y}\right)$$
$$-\frac{1}{2\rho^{(0)}c_p}\sqrt{\frac{\gamma p^{(0)}}{\rho^{(0)}}}\left(\sqrt{\gamma\rho^{(0)}p^{(0)}}\frac{\partial u^{(0)}}{\partial \xi}+\frac{\partial p^{(1)}}{\partial \xi}\right)+O\left(M^2\right). \tag{3.3}$$

An alternative non-reflecting condition can then be written by applying the non-reflecting condition of Hedstrom (Hedstrom 1979) to the *acoustic components* of the characteristic amplitudes (Prosser 2004);

$$\left(\sqrt{\gamma\rho^{(0)}p^{(0)}}\frac{\partial u^{(0)}}{\partial \xi}-\frac{\partial p^{(1)}}{\partial \xi}\right)=0. \tag{3.4}$$

Substituting this equation into equation 3.3, leads to

$$L_1 = L_4 - MT^{(0)}\sqrt{\frac{\rho^{(0)}}{\gamma p^{(0)}}}\left(\frac{1}{\mathrm{Re}}\left(\frac{\partial \tau_{yx}^{(0)}}{\partial x}+\frac{\partial \tau_{yy}^{(0)}}{\partial y}\right)+u_b\frac{\partial u^{(0)}}{\partial x}-v\frac{\partial u^{(0)}}{\partial y}\right)$$
$$-\left(\gamma-1\right)T^{(0)}\frac{\partial u^{(0)}}{\partial \xi}. \tag{3.5}$$

Thus, the problem applying the non-reflecting condition devolves into one of calculating $\partial u^{(0)}/\partial\xi$; the flow divergence on the acoustic scales. This may be accomplished in practical terms by considering the leading order equation for pressure:

$$\frac{\partial p^{(0)}}{\partial t}+\gamma p^{(0)}\nabla_x\cdot\mathbf{u}^{(0)}=\frac{1}{\mathrm{Re}\,\mathrm{Pr}}\nabla_x\cdot\left(\lambda^{(0)}\nabla_x\cdot T^{(0)}\right). \tag{3.6}$$

$\partial u^{(0)}/\partial\xi$ can thus be calculated by a two step process. The first step is to calculate numerically $\nabla_{\tilde{x}}\cdot\mathbf{u}$, the *as-is* flow divergence. Then, from equation 3.6, the constancy of the thermodynamic pressure imposes $\nabla_x\cdot\mathbf{u}^{(0)}=\frac{1}{\mathrm{Re}\,\mathrm{Pr}}\nabla_x\cdot\left(\lambda^{(0)}\nabla_x\cdot T^{(0)}\right)$. Hence the numerically calculated divergence satisfies

$$\nabla_{\tilde{x}}\cdot\mathbf{u}-\frac{1}{\mathrm{Re}\,\mathrm{Pr}}\nabla_x\cdot\left(\lambda^{(0)}\nabla_x\cdot T^{(0)}\right)=M\left(\frac{\partial u^{(0)}}{\partial\xi}+\frac{\partial v^{(0)}}{\partial\theta}\right)+O\left(M^2\right). \tag{3.7}$$

The second step is to assume that all acoustic waves incident on a boundary approach normally, implying $\partial v^{(0)}/\partial\theta=0$. This step is consistent with the spirit of the original LODI/NSCBC and other characteristic approaches; future work will concentrate on generalising the treatment to include acoustic waves approaching the boundary obliquely. Recalling the definition $a=M^{-1}\left(\gamma p/\rho\right)^{\frac{1}{2}}$—and with a slight abuse of notation—the required boundary conditions *in fully dimensional form* can be written as

$$L_1 = L_4+\frac{\left(\gamma-1\right)T}{a}\left(v\frac{\partial u}{\partial y}-u_b\frac{\partial u}{\partial x}-\left(\frac{\partial \tau_{yx}}{\partial x}+\frac{\partial \tau_{yy}}{\partial y}\right)\right)$$
$$-\quad\left(\gamma-1\right)T\frac{\partial u^{(0)}}{\partial\xi}, \tag{3.8}$$

where

$$\frac{\partial u^{(0)}}{\partial\xi}=\left(\frac{\partial u}{\partial x}+\frac{\partial v}{\partial y}\right)-\left(\frac{\partial}{\partial x}\left(\lambda\frac{\partial T}{\partial x}\right)+\frac{\partial}{\partial y}\left(\lambda\frac{\partial T}{\partial y}\right)\right). \tag{3.9}$$

If the flow is cold, then it is straightforward to show that $T^{(0)} = const.$, and the thermal conduction term can be dropped from the preceding equaition for $\partial u^{(0)}/\partial \xi$. We note that the molecular viscosity does not have an influence in calculating the $\partial u^{(0)}/\partial \xi$ term; this is due to viscosity only having a second order effect in the pressure transport equation.

4. Non reflecting viscous inflow conditions

The treatment of the inflow boundary conditions depends very much on the complexity of the field on the inlet plane. If the flow field is steady and has an analytic structure, the methods of the previous sections may be used to define non-reflecting conditions in a straightforward manner. If the incoming flow is turbulent, then a more sophisticated treatment is required.

For the turbulent inflow case, we have retained the method outlined in (Prosser 2004). We suppose that the simulation can be broken into two components: The *active* solution (for which we are seeking boundary conditions), and the precomputed *frozen* solution. The incoming characteristics required for the active solution are derived from the frozen solution, and convected across the inflow boundary.

In the precomputed solution, the periodic boundary conditions are usually employed, and these preclude the requirement for explicit conditions on the viscous fluxes (or indeed, any other terms). For open flow problems, we usually require the specification of some condition on the viscous fluxes. Hence, there is an inconsistency in the balancing of characteristics between the frozen solution and the active solution. We have as yet been unable to find a consistent way of matching the viscous effects between the two solutions. For a cold flow problem, the resulting pressure disturbances arising from this discrepancy should be small, as all momentum transport effects are of $O\left(M^2\right)$ in the pressure transport equation. If there are significant conduction effects—such as may be found when a flame approaches an inflow—then this error could grow to $O\left(1\right)$. Future work will concentrate on achieving a better consistency between frozen and active solutions, and will also examine methods of allowing evolving precomputed solutions to enter the active domain.

5. Results

5.1. *The code*

The boundary conditions described in this paper have been implemented in a code originally developed at UMIST. The code is parallel and is able to deal with any given chemical reaction mechanism. The code has been designed to work with a suite of numerical schemes, ranging from compact and explicit finite differences, to Chebyshev spectral methods and non-uniform high order discretisations. For this work, a uniform explicit fourth order approximation was used for spatial derivatives, and a minimal storage third order Runge-Kutta method developed by Wray (Wray 1990) was used for temporal integration. For all of the results that follow, the discretisation was based on a grid of 128×128 grid points, and ran on two processors on a SGI Origin 2000.

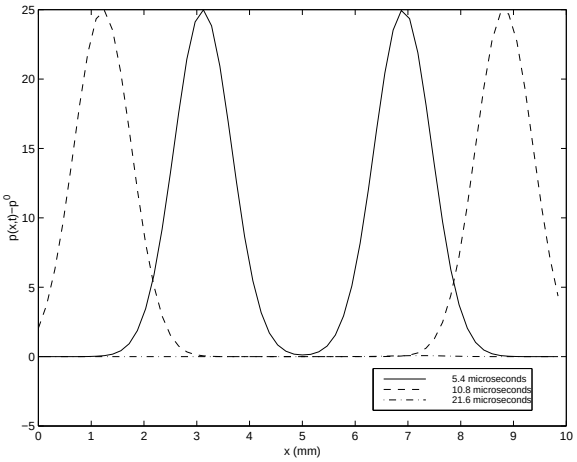

FIGURE 1. Sectional elevation of the flow field, showing the evolution of the acoustic pressure with time.

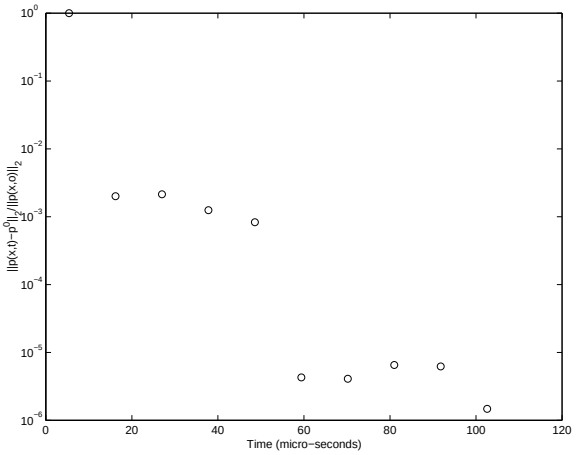

FIGURE 2. 2−norm of the evolving dynamic pressure field—laminar flow

5.2. *Non-reflecting behaviour*

Figure 1 shows the evolution of a pressure pulse in a domain 10mm square, comprising a steady flow of air with a uniform motion of 2m/s. The initial pressure field is given by

$$p'(\mathbf{x},t) - p^{(0)} = 2\exp\left(-\left(0.13(x-\frac{1}{2})\right)^2\right) \qquad -5\times10^{-3} \le x,y \le 5\times10^{-3}. \quad (5.1)$$

The simulation uses the boundary conditions developed above and incorporates the effects of viscosity and thermal conduction. This test is designed to demonstrate the non-reflective character of the boundary condition treatment. As can be seen, the pressure waves leave both the inflow and outflow boundaries smoothly. Figure 2 gives the time history of the 2-norm of the acoustic pressure: $\left|\left|p(\mathbf{x},t) - p^{(0)}\right|\right|_2 / \left|\left|p(\mathbf{x},0)\right|\right|_2$. We note that after 1 acoustic transit time ($O(l_0/a_0) \simeq 30\mu s$, here), the magnitude of the acoustic mode has dropped to 0.1% of the initial condition. After subsequent multiples of the acoustic transit time, the magnitude of the acoustic mode drops to 0.001%, and 0.0001%,

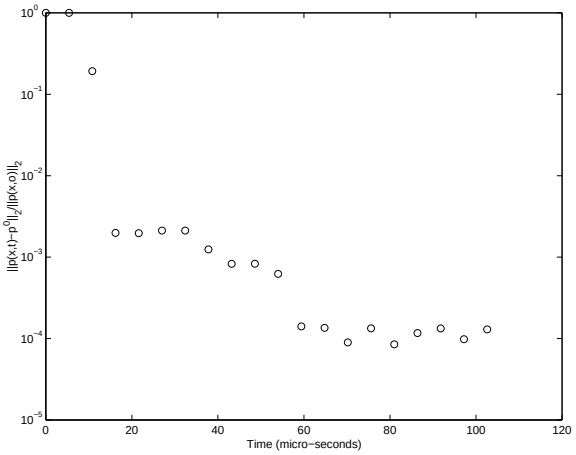

FIGURE 3. Evolution of the normalised pressure difference for the turbulent, acoustically perturbed solution.

respectively. The initial 0.1% reflection arises from the second order influence of the mean convection speed. The inclusion of a second order term in the non-reflecting criteria improves the performance of the boundary conditions further. This will be further explored in a future paper.

5.3. *Cold turbulence*

The second problem to be studied using the new boundary conditions is that of cold two-dimensional, viscous turbulence. The initial conditions for this flow were generated using the methods described by Rogallo (Rogallo 1981). The turbulent velocity fluctuations were calculated such that the resultant energy spectrum satisfied

$$E(k) = \begin{cases} \frac{72}{\pi}\frac{k}{k^4+6^4} & k \leq k_{\max} \\ 0 & k \geq k_{\max} \end{cases} \tag{5.2}$$

$k_{\max}$ was set for this study at 12, a subsequent normalization of the energy spectrum produced a turbulence RMS intensity of 0.1m/s (5% of the mean flow speed for this case). The resultant flow field contains a range of length and time scales characteristic of turbulence, but one that is readily resolved using a low resolution grid of 128×128 grid points. This last comment is particularly aimed at the one sided schemes used at the inflow/outflow boundaries; these often have a lower formal order of accuracy, and a much poorer spectral resolution, than symmetric internal constructions. The mean velocity for this investigation was set at 2.0m/s and the physical size of the domain was set at 10mm×10mm.

The simulation was run twice. The first simulation evolved from the set of initial conditions *without* the pressure pulse, and provided the evolving benchmark pressure field $p_{ref}(\mathbf{x}, t)$. The second simulation shared the same inertial features as the benchmark solution, but also included the pressure perturbation given by equation 5.1. The idea is that the two simulations should share the same time dependent inertial behaviour, but the second simulation should have an additional acoustic component. If the non-reflecting boundary conditions work correctly, this component should leave the domain after half an acoustic transit time. The two solutions should thereafter evolve identically, and the

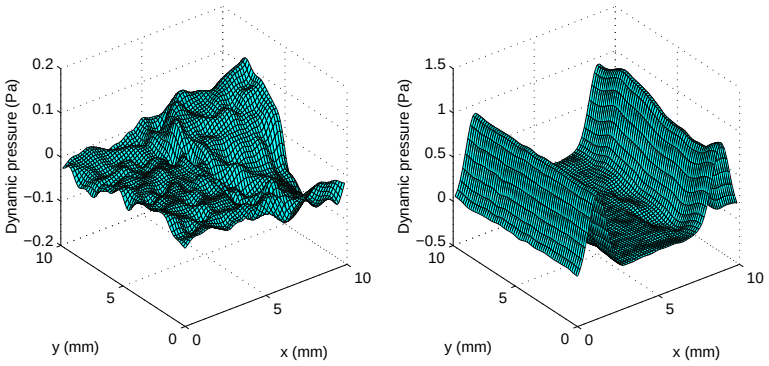

FIGURE 4. Comparison between dynamic pressure surfaces for the reference simulation and acoustically perturbed simulation after an elapsed simulation time of $16.2\mu s$

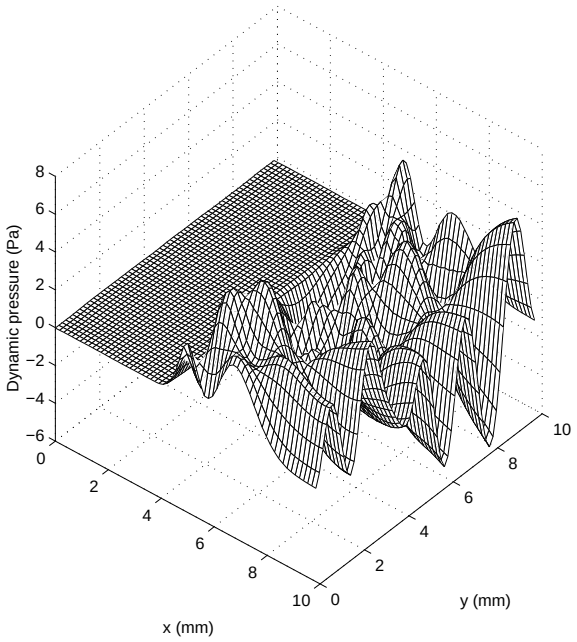

FIGURE 5. Propagation of spurious acoustic waves into the domain from the NSCBC outflow boundary. Elapsed simulation time = $16.2\mu s$.

difference between them, embodied by a normalised pressure difference

$$\frac{||p(\mathbf{x},t) - p_{ref}(\mathbf{x},t)||_2}{||p(\mathbf{x},0)||_2}, \tag{5.3}$$

should vanish.

Figure 3 shows a logarithmic plot of the time history of the normalised pressure difference (equation 5.3). Figures 4a and b show the dynamic pressure surfaces for the reference solution and the perturbed solution at an elapsed simulation time of $16.2\mu s$. In figure 4b, we can see the pressure pulses are just leaving the domain via the inlet and outlet boundaries. It is at this time that the large reduction in normalised pressure difference,

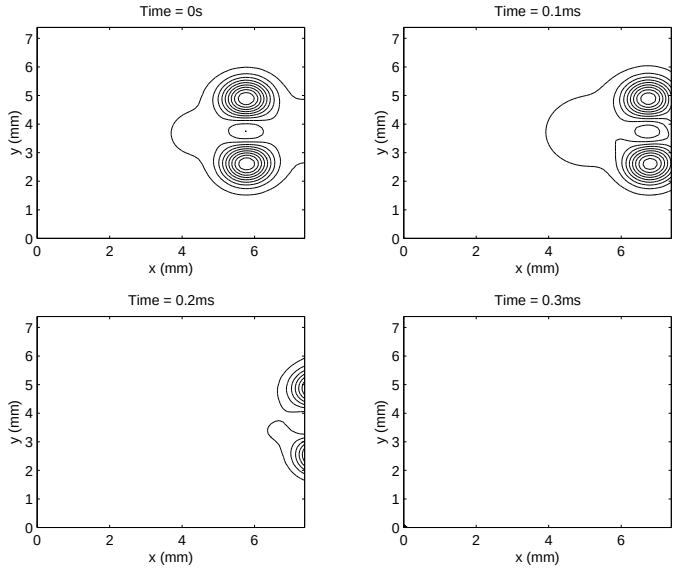

FIGURE 6. Pressure contour plots of twin co-rotating vortices approaching a revised non-reflecting outflow. Centres of vortices are heated to 600K.

visible in figure 3 takes place. Finally, figure 5 shows the pressure field obtained from a simulation also at an elapsed simulated time of $16.2\mu s$, but this time using NSCBC boundary conditions. As can be seen, spurious pressure oscillations from the outflow boundary conditions have begun to propagate upstream at the local sound speed, and are well on their way to swamping the pressure field induced by the dynamics alone.

The simulations using the new boundary conditions were allowed to continue to run for an additional 45×10^3 time steps, which corresponds to 1 flow transit time (defined as l_0/u_0). At the end of this extended run, no significant errors in the pressure field were observed, and the dynamic pressure variations remained bounded essentially by the kinetic energy of the turbulence.

5.4. *Co-rotating hot vortices*

Figures 6a-d show the pressure evolution for 2 co-rotating vortices leaving the computational domain. This configuration was chosen because there is an inertial evolution in the flow, as well as acoustic transients arising from the initial conditions. The mean flow speed is set to 10m/s, and the two vortices are initialised using a stream function

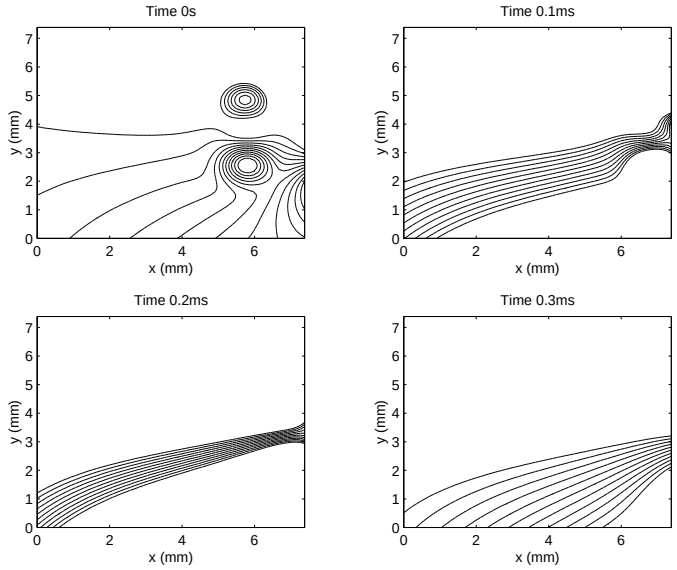

FIGURE 7. Pressure contour plots of twin co-rotating vortices approaching a standard non-reflecting outflow. Centres of vortices are heated to 600K.

approach defined initially on a domain $\widetilde{\Omega} = \{\widetilde{x}, \widetilde{y} : 0 \leq \widetilde{x} \leq 1, 0 \leq \widetilde{y} \leq 1\}$,

$$\begin{aligned}
\psi &= C\left(\exp\left(-\frac{r_a^2}{2r_v^2}\right) + \exp\left(-\frac{r_b^2}{2r_v^2}\right)\right) + u_b y \\
r_a &= \left(\left(\widetilde{x}+0.5\right)^2 + \left(\widetilde{y}-0.15\right)^2\right)^{\frac{1}{2}} \\
r_b &= \left(\left(\widetilde{x}+0.5\right)^2 + \left(\widetilde{y}+0.15\right)^2\right)^{\frac{1}{2}} \\
u &= \frac{\partial \psi}{\partial \widetilde{y}} \\
v &= -\frac{\partial \psi}{\partial \widetilde{x}} \\
T &= 300\left(1 + \exp\left(-\frac{r_a^2}{2r_v^2}\right) + \exp\left(-\frac{r_b^2}{2r_v^2}\right)\right).
\end{aligned} \tag{5.4}$$

C is the vortex strength, u_b is the mean velocity and r_v is a characteristic radius. For this simulation, C was set at $0.5\mathrm{m}^2/\mathrm{s}^2$, r_v was set at 8% of the domain size and the mean velocity u_b was set at 10m/s. The physical flow domain is 7.5mm square, and a linear mapping was used to relate quantities in the physical domain to the initial conditions calculated by equations 5.4a-f. The pressure was assumed initially to be constant, and the density was calculated using the thermal equation of state. The thermal conductivity was calculated using (Echekki & Chen 1996)

$$\lambda = 2.58 \times 10^{-5} \times c_p \left(\frac{T}{300}\right)^{0.7} \tag{5.5}$$

As the flow field has a simple far field structure, the standard NSCBC treatment was used for the transverse directions. For the inlet a fixed velocity, non reflecting condition

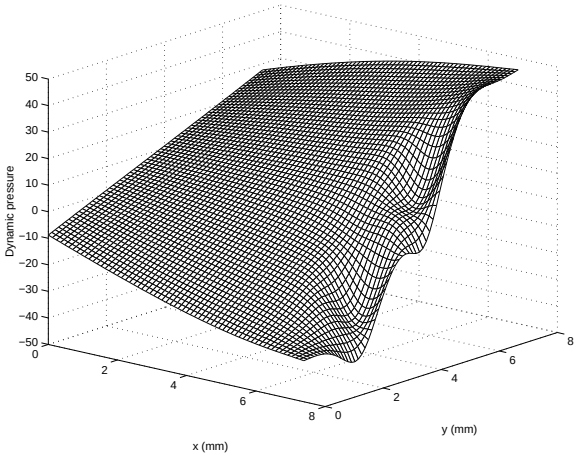

FIGURE 8. Dynamic pressure surface for hot vortices crossing NSCBC boundary conditions. Surface corresponds to contour plot 7c.

was imposed (Prosser 2004). As can be seen from figures 6a-d, there is no appreciable distortion arising from the boundary conditions. Figures 7a-d show the evolution of the pressure field for the problem when normal NSCBC boundary conditions are applied. In figure 7a-d, the contours have been restricted to the same range as those in figures 6a-d. Figure 8 shows the pressure surface corresponding to contour plot 7c. We note the significant transverse pressure variation across the entire domain, arising as a result of the pollution induced by the old boundary conditions.

6. Large-Eddy Simulations

In the next step, we want to apply the boundary condition to Large-Eddy Simulations (LES). In LES, the filtered Navier-Stokes equations are solved, which means in turbulent flows the large scale motions of turbulence are resolved in space and time on a given mesh, while the smaller scales are modeled using an eddy viscosity approach.

Here, we are using a structured compressible LES flow solver developed by Pierce (Pierce & Moin 1998) and Wall (Wall *et al.* 2002), which uses a second-order finite-volume scheme on a staggered grid (Akselvoll & Moin 1996). The sub-grid stresses are approximated by a dynamic procedure (Germano *et al.* 1991; Moin *et al.* 1991). The pressure and density field are determined by solving the Helmholtz equation and the time-step was set to satisfy the acoustic CFL condition.

Using the LES flow solver, the test-case described in section 5.4 was computed. The LES mesh size was $128 \times 128 \times 8$ nodes. The discretization in z-direction was intentionally left coarse in order to compute a quasi-2D flow. The mesh is concentrated near the path of the vortices. In transverse direction non-slip wall conditions were applied.

Fig. 9 shows the pressure distribution at the outlet cross section at the instant of maximum distortion. We note that the pressure distortion is much more attenuated using Eq. (3.8).

We performed additional LES computations without a subgrid model in order to assess the effect of the additional viscous terms of the subgrid model. The results of these computations were virtually indistinguishable from the previous results, which means that

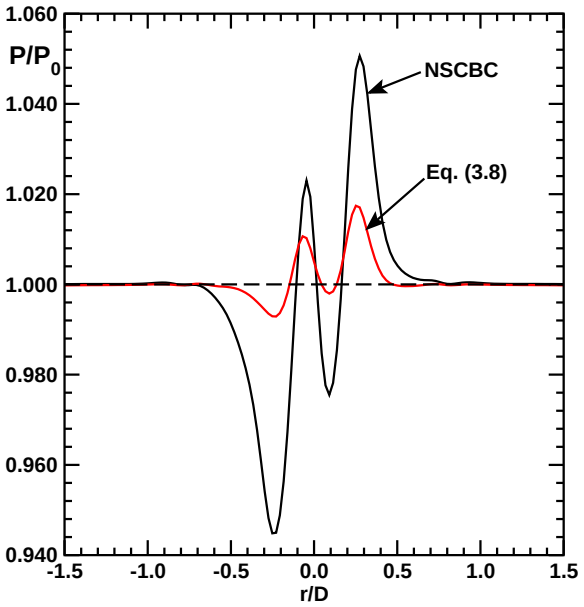

FIGURE 9. LES computation of co-rotating vortices passing outflow: cross-section pressure distribution at the instant of maximum pressure distortion.

for the chosen test case, the influence of the subgrid model on the boundary conditions is neglectable.

7. Conclusions

A procedure to improve the specification of time dependent boundary conditions for viscous flows has been described. The approach is based on a low Mach number expansion of the governing equations, and is an extension of a method originally developed for inviscid flows. The incorporation of thermal conduction and viscosity into the new boundary conditions are shown to have leading and second order effects, respectively. The new approach provides a significantly better treatment of the pressure field—both at inflow and outflow boundaries—than the previous characteristics based methods. The new treatment is able to deal with flows comprising inhomogeneous high temperature regions without inducing spurious effects. The scheme appears to be stable for long time integration periods.

A number of areas have emerged during the course of this investigation that require further analysis. Firstly, it can be shown that a modification to equation 3.3 to include second order effects provides a less reflective boundary condition. The effects on stability of this modification has yet to be established for long time scale integrations. Secondly, no viscous boundary conditions were imposed during the course of these simulations, other than the explicit coupling of the viscous fluxes to the inertial terms via the characteristics, as seen in equation 3.3. It is not clear at this stage whether the coupling can be interpreted as a type of viscous condition in the form recommended by Dutt (Dutt 1988), although the practical long term stability of the calculations presented here do provide grounds for cautious optimism. Thirdly, the extension of the asymptotic methods to reacting flows is straightforward and will be examined in a forthcoming paper.

Finally, the new approach still suffers from the thermodynamic pressure drift found in other characteristics based methods. This drift has been identified with the failure of the numerical schemes properly to enforce a leading order solenoidal constraint on the velocity field, when formally the flow should be divergence free. Future work will examine the improvement of numerical methods and/or boundary conditions to reduce the drift, without recourse to the pressure-at-infinity condition proposed by Strikwerda (Strikwerda 1977), which has a tendency to introduce Nyquist frequency oscillations into the flow field.

8. Acknowledgments

We thank Clifton Wall for providing the compressible LES flow solver.

REFERENCES

AKSELVOLL, K., & MOIN, P. 1996 Large-eddy simulation of turbulent confined coannular jets. *J. of Fluid Mech.*, **315**, 387–411.

BAUM, M., POINSOT, T.J. & THÉVENIN, D. 1994 Accurate Boundary Conditions for Multicomponent Reactive Flows. *J. Comp. Phys.*, **116**, 247–261.

DUTT, P. 1988 Stable Boundary Conditions and Difference Schemes for Navier-Stokes Equations. *SIAM J. Num. Anal.*, **25**, 245–267.

ECHEKKI, T.& CHEN, J.H. 1996 Unsteady Strain Rate and Curvature Effects in Turbulent Premixed Methane-Air Flames. *Combustion and Flame*, **106**, 184–202.

GERMANO, M., PIOMELLI, U., MOIN, P. & CABOT, W. 1991 A dynamic subgrid-scale eddy viscosity model. *Phys. Fluids* A **(3)**, 1760-1765.

GRINSTEIN, F.F. 1994 Open Boundary Conditions in the Simulation of Subsonic Turbulent Shear Flows. *J. Comp. Phys.*, **115**, 43–55.

HEDSTROM, G.W. 1979 Nonreflecting Boundary Conditions for Nonlinear Hyperbolic Systems. *J. Comp. Phys.*, **30**, 222–237.

HESTHAVEN, J.S. 1998 On the Analysis and Construction of Perfectly Matched Layers for the Linearized Euler Equations. *J. Comp. Phys.*, **142**, 129–147.

HU. F.Q. 1996 On Absorbing Boundary Conditions for Linearized Euler Equations by a Perfectly Matched Layer. *J. Comp. Phys.*, **129**, 201–219.

KLEIN, R. 1995 Semi-Implicit Extension of a Godunov-Type Scheme Based on Low Mach Number Asymptotics I: One Dimensional Flow. *J. Comp. Phys.*, **121**, 213–237.

MAJDA, A. AND SETHIAN, J. 1985 The derivation and Numerical Solution of the Equations for Zero Mach Number Combustion. *Combust. Sci. and Tech.*, **42**, 185–205.

MCMURTRY, P.A., JOU, W.H., RILEY, J.J. & METCALFE, R.W. 1986 Direct Numerical Simulations of a Reacting Mixing Layer with Chemical Heat Release. *AIAA Journal*, **24**, 962–970.

MOIN, P., SQUIRES, K., CABOT, W. & LEE, S. 1991 A dynamic subgrid-scale model for compressible turbulence and scalar transport. *Phys. Fluids*, A **(3)**, 2746-2757.

NICOUD, F. 1999 Defining Wave Amplitude in Characteristic Boundary Conditions. *J. Comp. Phys.*, **149**, 418–422.

PIERCE, C. D. & MOIN, P. 1998 Large eddy simulation of a confined coaxial jet with swirl and heat release. *AIAA Paper* 98-2892.

POINSOT, T.J. & LELE, S.K. 1992 Boundary Conditions for Direct Simulations of Compressible Viscous Flows. *J. Comp. Phys*, **101**, 104–129.

PROSSER, R. 2004 Improved Boundary Conditions for the Direct Numerical Simulation of Turbulent Subsonic Flows I: Inviscid Flows. *submitted to J. Comp. Phys.*

ROGALLO, R. 1981 Numerical Experiments in Homogeneous Turbulence. *NASA Technical Report 81315*, NASA Ames.

RUDY, D.H. AND STRIKWERDA, J.C. 1980 A Nonreflecting Outflow Boundary Condition for Subsonic Navier-Stokes Calculations. *J. Comp. Phys.*, **36**, 55–70.

RUDY, D.H. AND STRIKWERDA, J.C. 1981 Boundary Conditions for Subsonic Compressible Navier-Stokes Calculations. *Comput. Fluids.*, **9**, 327–338.

STRIKWERDA, J. C. 1996 Initial boundary value problems for incompletely parabolic systems. *Commun. Pure Appl. Math.* , **30**, 797–822.

SUTHERLAND, J.C. & KENNEDY, C.A. 2003 Improved boundary conditions for viscous, reacting, compressible Flows. *J. Comp. Phys.*, **191**, 502–524.

THEVÉNIN, D., BAUM, M. & POINSOT, T.J. 1996 Direct Numerical Simulation for Turbulent Reacting Flows. *Editions Technip, Paris*, 11–32.

THOMPSON, K.W. 1987 Time Dependent Boundary Conditions for Hyperbolic Systems. *J. Comp. Phys.*, **68**, 1–24.

TSYNKOV. S.V. 1998 Numerical solution of problems on unbounded domains. A review. *Appl. Numer. Math.*, **27**, 465–532.

VICHNEVETSKY, R. 1986 Invariance Theorems Concerning Reflection at Numerical Boundaries. *J. Comp. Phys.*, **63**, 268–282.

WALL, C., PIERCE, C.D. & MOIN, P. 2002 A Semi-implicit Method for Resolution of Acoustic Waves in Low Mach Number Flows. *J. Comp. Phys.*, **181**,2, 545–563.

WRAY A.A. 1990 Minimal Storage Time-Advancement Schemes for Spectral Methods. *unpublished*, NASA Ames Research Center.